

Intramolecular Proton Transfer of Glycine in Aqueous Solution Using Quantum Mechanics—Molecular Mechanics Simulations

Iñaki Tuñón and Estanislao Silla*

Departamento de Química Física, Universidad de Valencia, 46100 Burjasot, Valencia, Spain

Claude Millot, Marilia T. C. Martins-Costa, and Manuel F. Ruiz-López*

Laboratoire de Chimie Théorique, UMR CNRS-UHP No. 7565, Institut Nancéien de Chimie Moléculaire, Université Henri Poincaré—Nancy I, BP 239 54506 Vandoeuvre-lès-Nancy, France

Received: May 7, 1998

Molecular dynamics simulations within the density functional—molecular mechanics approach are used to investigate amino acid chemistry in aqueous solution. Equilibrium solvation effects are studied in both the neutral and zwitterionic forms of the glycine. Dynamic solvent effects on amino acid reactions in water are illustrated through the simulation of the fast conversion of neutral glycine to its zwitterionic form. The different factors contributing to the intramolecular proton transfer are analyzed from a dynamic point of view.

1. Introduction

Amino acid chemistry in aqueous solution has been the subject of a large variety of studies because of its importance in the understanding of proteins behavior.^{1–7} It is well-known that, while in the gas-phase amino acids exist as neutral forms, zwitterionic ones predominate in aqueous solution.¹ Since the 1970, many theoretical efforts have been devoted to interpreting this phenomenon.² Because of its small size and the existence of experimental data, glycine has been usually chosen as the prototype of amino acids in theoretical investigations. Several stable conformations have been found for the neutral form of glycine, and the corresponding geometries and relative energies have been thoroughly studied. Such results are quite interesting because of their implications in the description of protein structure.² By means of high-level *ab initio* calculations, it has been established that only the neutral form of glycine amino acid exists in the gas phase, the zwitterion being unstable under such conditions.³

Until now, theoretical studies of amino acids in solution have been mainly done in three distinct ways. The first one consists of the quantum mechanical calculation of the solute surrounded by a small number of water molecules. Following this approach, it has been recently shown^{4,5} that at least two water molecules are required to predict an energy minimum in the potential energy surface of glycine zwitterion. However, due to the long-range nature of electrostatic interactions, an accurate description of the conversion between neutral and zwitterionic forms would require the inclusion of several hundreds of water molecules into the quantum mechanical calculations, which is clearly prohibitive now, even at the semiempirical level. A second alternative is the combination of the quantum treatment of the amino acid with a dielectric continuum description of the environment.⁸ It has been recently shown^{5,6} that this methodology correctly predicts the zwitterion to be the predominant form of glycine in water. The main drawback of calculations based on continuum models is the lack of microscopic information, like the solvent structure around the solute. Moreover, one can

only reach a static description of reactive processes. Another possible approach to liquid state phenomena is offered by statistical methods such as Monte Carlo or molecular dynamics techniques. By means of these methods, a great number of solvent molecules can be treated, and the solvent structure around the solute is directly obtained. Several applications to glycine zwitterion in water have been reported.⁹ However, potential energy functions used in these methods are hardly adapted to investigate chemical processes involving bond breaking and forming. Some effort has been made to develop potentials and investigate the dynamic solvent effect of simple reactions such as ion association¹⁰ and S_N1 ^{11,12} and S_N2 ^{12,13} processes, for instance. An attractive approach is the empirical valence bond (EVB) method proposed by Warshel and Weiss,¹⁴ in which the reacting system is represented as a superposition of covalent and ionic forms. The Hamiltonian of the solute also includes the solvation energy. This model has allowed researchers to study the dynamics of a number of chemical and biochemical reactions, including the intramolecular proton transfer of glycine,⁷ and to demonstrate the major role played by fluctuations of the environment.¹⁵ In the last years, mixed quantum mechanical-molecular mechanics methods (QM/MM) have been developed,^{16–23} overcoming many of the limitations displayed by previous methods. In these methods, the full system, solute and solvent, is described at a molecular level but only a part of the system, limited normally to the reactants, is treated at a quantum mechanical level. The rest of the system is described classically by means of molecular mechanics potentials, point charges, van der Waals parameters, and so on. To save computational time, the first QM/MM implementations were carried out using semiempirical wave functions¹⁶ for the quantum subsystem. Now, *ab initio*¹⁸ and density functional (DF) techniques are also used.^{19,20} Though these latter methods require a greater computational effort, they allow a better description of chemical processes than semiempirical treatments. We have recently developed a DF/MM program that has allowed us to carry out Monte Carlo (MC)²⁰ and molecular dynamics

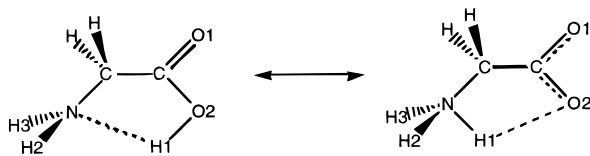


Figure 1. Neutral and zwitterionic forms of the glycine amino acid considered here for the constrained-solute DF/MM MD simulations in aqueous solution.

(MD)²¹ simulations of aqueous solutions as well as to study some reactions such as a low-barrier proton transfer²² and charge separation²³ processes in water. In refs 22 and 23, it was shown that this approach is a powerful tool for analyzing solvent effects on reactions and describing elementary chemical events in solution.

MD simulations within the combined DF/MM approach are, therefore, promising for the investigation of amino acid chemistry in aqueous solution. We illustrate this assertion below through the study of a simple but fundamental process: the fast conversion of neutral glycine to a zwitterionic species in water through intramolecular proton transfer favored by hydration.

2. Methodology

In our combined DF/MM MD study, the classical subsystem is composed of 212 water molecules, and the quantum subsystem is the glycine molecule. We used double- ζ quality basis sets including polarization functions on nitrogen and oxygen atoms with contractions: H(41), N(621/41/1), O(621/41/1), and C(621/41). The auxiliary basis sets for the electron density and exchange-correlation fit were (4;4) for hydrogen and (4,3;4,3) for the rest of the atoms. See program deMon²⁴ for details. Both local²⁵ and nonlocal²⁶ functionals were used for the exchange-correlation term. Lennard-Jones parameters for quantum atoms were taken from ref 27, and the TIP3P potential²⁸ was selected for the classical water molecules. Details on the computation of the coupled QM/MM term are given elsewhere.^{21,22} Analytical forces are obtained from the derivatives of the energy with respect to the positions of quantum nuclei and classical sites. Using these forces, one is able to integrate the corresponding equations of motion to obtain the new atom positions at $t' = t + \Delta t$. In this way, a trajectory of the full system can be followed. Simulations have been carried out at the NVT ensemble in a cubic box of 18.6-Å sides at 25 °C using the Nosé–Hoover algorithm.²⁹ Periodic boundary conditions and a cutoff distance of 9.0 Å have been applied. Quantum hydrogen atoms have the mass of deuterium. Calculations were carried out on a RS/6000 model 3BT SPECfp95 7.52. For the unconstrained simulation using the nonlocal, one step took about 1.8 min of CPU.

3. Results and Discussion

Simulations were initially carried out for fixed geometries of the neutral (NE) and zwitterionic (ZW) forms of glycine, in the conformations shown in Figure 1. These geometries were obtained from energy minimizations with a continuum model at the computational level employed in the simulations. Note that the conformation of the absolute minimum of the neutral form in solution is different from that in the gas phase, as discussed in ref 5. For these simulations, we used the VWN²⁵ local exchange-correlation functional. The whole system (quantum plus classical subsystems) was equilibrated during 35 ps using a time step of 1 fs. Afterward, averaging was carried out during 25 ps. The radial distribution functions (RDF) for nitrogen (N) and oxygen (O2) atoms taking part in the

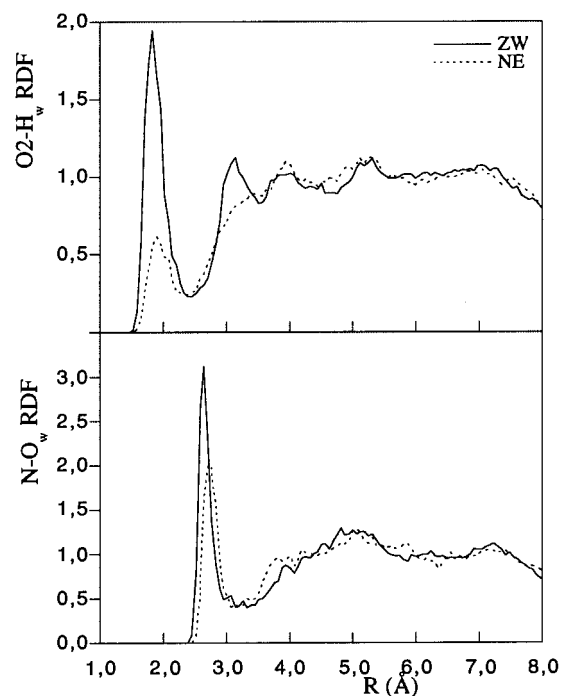


Figure 2. Radial distribution functions obtained for the neutral (···) and zwitterionic (—) forms of the glycine as obtained from constrained-solute DF/MM MD simulations in aqueous solution.

intramolecular hydrogen bond are shown in Figure 2 for the two forms of the amino acid. The curves show a more structured first solvation shell around the N and O2 atoms in the case of the zwitterion. The first peak of the nitrogen RDF appears at 2.64 and 2.76 Å for the zwitterion and the neutral species, respectively. In the oxygen atom RDF, the first peak lies at 1.83 and 1.90 Å for the same species. The coordination numbers, obtained from integration of the RDFs up to the first minima, show that approximately three solvent molecules (2.8) constitute the first solvation shell of the nitrogen atom in the zwitterionic form and only two (2.1) in the neutral one. The coordination number for the O2 oxygen atom is about two (2.3) in the zwitterion and one (1.0) in neutral glycine. Radial distribution functions for other atoms show only minor changes between the neutral and zwitterionic forms. The averaged dipole moments obtained along the simulations are 14.8 and 9.6 D for the zwitterion and the neutral glycine, respectively. This change in polarity when passing from the neutral to the zwitterionic form (more than 5 D) originates a remarkable difference in the averaged solute–solvent interaction energy equal to -77.1 kcal/mol. Of course, the large value of this quantity is responsible for the stabilization of the zwitterion in solution.

We consider now the conversion of this neutral conformer to the zwitterionic form of glycine through the effect of solvation. To study the associated proton transfer process, we arbitrarily chose an equilibrated configuration for neutral glycine as the starting point for the MD simulation. Along the MD trajectory, the internal coordinates of the quantum system (glycine) are unconstrained. Despite the considerable increase of the computational cost, in this case we added Becke–Perdew²⁶ density gradient corrections to the exchange-correlation term because of the important changes in the electron density when passing from the neutral to the zwitterionic form of the glycine. Before starting the simulation, the system was further equilibrated with the new potential, relaxing the geometry of the glycine except for the O2–H1 distance, which was kept fixed. The molecular dynamics simulation was run during a

total time of 2 ps using a time step of only 0.4 fs. The computation is repeated for a series of different initial configurations homogeneously distributed along the constrained simulation. Only one of these trajectories is described in detail here to illustrate the dynamics of the process. For each trajectory, after a few femtoseconds, the system systematically evolved toward the formation of the zwitterionic glycine system, as we show below. This indicates that the activation barrier for proton transfer starting from the neutral conformation of glycine considered above is necessarily very small or lacking. In other words, that conformation of neutral glycine is a very shallow minimum in the potential energy surface. Previous *ab initio* free energy computations⁵ including correlation in a continuum model solution had predicted this conformation to be more stable than the gas-phase conformation of glycine (with NCCO2 and CC2OH1 dihedral angles equal to 180°) by 2.7 kcal/mol and to have a very small barrier (1.9–2.4 kcal/mol) for proton transfer. The latter point is actually confirmed by our simulation. The interconversion between the two minima of neutral glycine has been evaluated in the present work using an ellipsoidal cavity model similar to that used before⁵ but using a computational level comparable to that employed in our simulation (density functional with gradient corrections, 6-31G* basis set). We have predicted an activation free energy barrier of 10.9 kcal/mol for conversion from the gas-phase minimum to that suitable for proton transfer. This value is of the same order of magnitude as the available experimental data for the barrier for conversion of neutral to zwitterionic glycine, which amounts to 14.4 kcal/mol from the zwitterion (i.e., around 7 kcal/mol from the neutral form).³⁰ Therefore, one may suggest that the proton transfer mechanism corresponds to a two-step process: reorientation of the amino and acid groups, starting from the gas-phase neutral conformation, followed by a practically barrierless proton transfer. Thus, the essential activation energy for obtaining a zwitterion would not be originated by proton transfer itself but by a conformational change of the neutral glycine.

Connected with the previous discussion, it is opportune to make some comments on a recent study of the free energy profile for proton transfer in glycine by means of a combined EVB molecular dynamics study.⁷ In this work, the authors computed the potential of mean force along a reaction path that was defined in the gas phase through Hartree–Fock computations at the 6-31+G* level. The starting conformation of neutral glycine was not the most stable one in the gas phase but that suitable for proton transfer, i.e., the same that we have considered in our simulation. A free energy barrier of 8.5 kcal/mol has been found. This value contrasts with our conclusion above that proton transfer (from this conformation) should be almost barrierless. The explanation is nevertheless simple. The EVB potential was parametrized using the Hartree–Fock results, which overestimates the barrier quite substantially. Indeed, in previous work,⁵ the free energy barrier at Hartree–Fock and MP2 levels was predicted to be 11.0 and 2.4 kcal/mol, respectively. Clearly, the correlation energy is extremely important in this reaction and cannot be neglected. One may notice also that the difference in solute–solvent interaction energy between the neutral and zwitterionic forms was predicted to be 43.7 kcal/mol in the above EVB study, which is much smaller than the 77.1 kcal/mol predicted here at the nonlocal level or the value reported by Clementi et al.,^{9a–c} who found 86.4 kcal/mol.

In Figure 3, we show the geometrical and the electronic properties evolution during the conversion process for the selected trajectory. In the upper plot, one can observe the

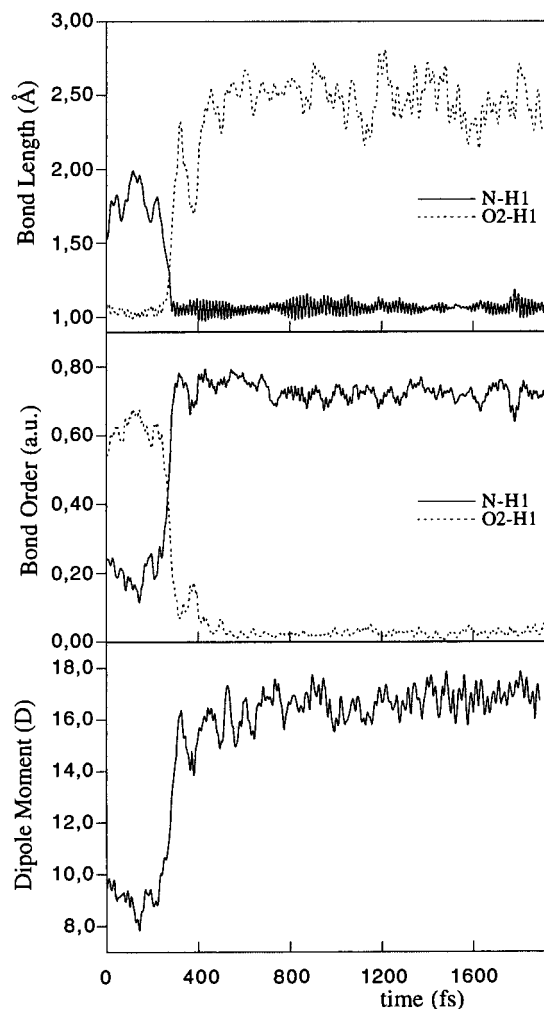


Figure 3. Results of the combined DF/MM MD simulation for neutral to zwitterion glycine conversion process. From top to bottom: bond lengths (N–H1, —; O2–H1, ···), bond orders (N–H1, —; O2–H1, ···), and dipole moment.

evolution of the two principal bond lengths (N–H1, O2–H1) involved in the process. At the beginning, the H1–O2 distance shows high-frequency vibrations, as expected for such a bond (period of about 15.5 fs, i.e., 3000 cm^{-1} when corrected for deuterium mass effect), whereas the H1–N distance displays large oscillations, as also expected for a nonbonded atom pair. The proton transfer from oxygen to nitrogen atoms takes place at approximately 260 fs after relaxing the quantum system constraints. Afterward, the situation is reversed, and the formed H1–N bond displays high-frequency vibrations (period of about 14.3 fs, i.e., 3300 cm^{-1} when corrected for deuterium mass effect). The second plot shows the evolution of Mayer bond orders:³¹ the H1–O2 bond decreases from about 0.6 to nearly 0.0, and the H1–N bond order changes from about 0.2 to more than 0.7. Note that the relative strength of the H1–O2 and H1–N bonds (in terms of bond order) is consistent with the relative value of the vibration frequencies. In the last plot, the conversion process is monitored in terms of the variation of the dipole moment of the glycine amino acid. The dipole moment changes approximately from 9 to 16 D after proton transfer.

Four geometry snapshots of the interconversion process corresponding to $t = 200, 270, 405,$ and 440 fs are shown in Figure 4. In the first snapshot, glycine is still in the neutral form. The number of water molecules hydrogen bonded to

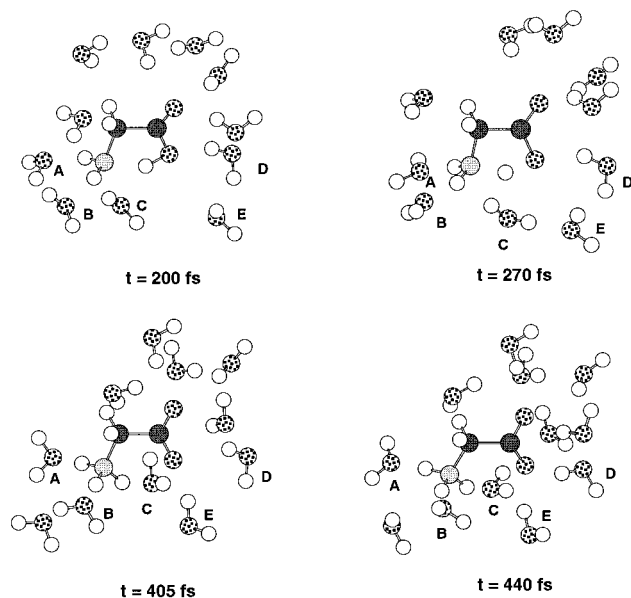


Figure 4. Instantaneous configurations of glycine and closest water molecules obtained from the DF/MM MD simulation at $t = 200$, 270, 405, and 440 fs. For clarity, water molecules that are more than 3.5 Å from any non-hydrogen atom of glycine have been removed.

nitrogen and oxygen atoms matches the coordination number obtained from the RDFs. Thus, two water molecules (A and B) form hydrogen bonds with the hydrogens of the nitrogen atom, while only one (D) is hydrogen bonded to the O2 oxygen. There are two other water molecules (C and E) which seems to stabilize electrostatically the acid hydrogen atom (H1). The second snapshot was chosen in the region of the proton transfer. The proton (H1) is just jumping from the oxygen to the nitrogen atom. The description of the first solvation shell around the nitrogen (N), oxygen (O2), and proton (H1) remains essentially unaltered. In the third snapshot, the glycine zwitterion is already formed, but the solvent is not yet fully relaxed around it. The A and B water molecules are now closer to the nitrogen atom, and an additional water molecule placed between them appears in the figure. Two water molecules (D and E) are now clearly hydrogen bonded to the O2 oxygen atom. These changes are related to the local charges appearing on nitrogen and oxygen atoms. Water molecule C has followed the proton and is now placed between the transferred proton and the oxygen. The last snapshot corresponds to a partially relaxed solvent structure around the glycine zwitterion. The main difference with respect to the previous snapshot is that the C water molecule is now properly oriented between the transferred proton (H1) and the O2 oxygen atom so that it is involved in two hydrogen bonds. Such hydrogen bonds are expected to be strengthened through cooperative effects.³² This water molecule remains in this position during the rest of the simulation time. The detailed analysis of the trajectory showed the presence of a second bridging water molecule incidentally. The C water molecule is strongly attached to the glycine zwitterion and induces important geometrical distortions in the amino acid. The averaged values for the H1NCC and O2CCN dihedral angles calculated after the zwitterion formation are 15 and -42° , respectively. An ab initio HF/6-311+G** calculation of an equivalent zwitterion–water molecule complex gave similar results, 7 and -35° , respectively.^{5a} The presence of a water molecule between O2 and H1 in the zwitterion suggests that the reverse proton transfer (to form the neutral species) could take place through an assisted mechanism in which the water molecule would act as a bifunctional catalyst. However,

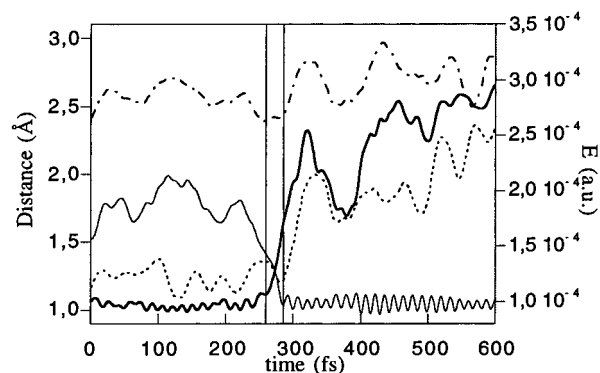


Figure 5. Plot of the N–H1 (—), O2–H1 (bold line), and N–O2 (···) distances and a solvent electric field component (— · —, see text) along the first 600 fs of the simulation.

previous studies seem to indicate that the intermolecular proton transfer has an activation energy larger than the intramolecular one.⁵ Thus, to observe the reverse proton transfer, the water molecule should be removed, which has not been observed in our simulation and would surely require a much larger simulation time.

The influence of the solvent dynamics on proton transfer has been investigated in detail through DF/MM MD simulations.²² To analyze the coupling between solute and solvent dynamics it is convenient to define a global solvent coordinate. For this purpose we have selected the electric field created by the solvent in the solute's region. We evaluate this field at the glycine's centroid of charges along the axis defined by the nitrogen and carbon atom of the acid group, chosen as approximative centers of positive and negative charges. In Figure 5, we show the evolution of the two geometrical parameters that describe the process: the O2–H1 and N–H1 bond lengths, together with the N–O2 distance and the solvent electric field along the first 600 fs of the simulation. The two vertical lines indicate the times for “beginning” and “end” of the proton transfer, which are simply defined as the times at which the oxygen (nitrogen) proton distance reaches the last (first) minimum before (after) the reaction. The transfer is very fast (about 30 fs) and takes place in a nearly frozen environment (it must be remembered here that, as usual in this kind of simulations, we use deuterium masses for quantum hydrogens). In fact, solvent relaxation begins after the proton transfer, and 200 fs later the solvent electric field approaches its new equilibrium value (about 2.5×10^{-4} au).

Considering the previous comments, one may expect solvent fluctuations to play an important role in process dynamics. The role of solvent fluctuations on proton transfer processes has been discussed before. Kurz and Kurz³³ proposed different mechanisms for proton transfer in solution representing extreme situations in which the solvent may be basically considered either as a thermal bath equilibrated with the solute along the reaction coordinate or as a fluctuating environment which may or may not assist the chemical process. According to this work, when the activated complex does not have an equilibrium environment, the deviation of solvent configuration from its equilibrium state is expected to be toward that configuration which is appropriate for an internal structure in which the proton is half transferred. This model is then related to the Marcus theory of proton transfer reactions.³⁴ On the other hand, molecular dynamics simulations with the EVB method have made it possible to demonstrate the active role played by the solvent and the importance of its fluctuations in proton transfer reactions. Basically, the rate of the reaction has been shown

to be related to the product of the probability that the solvent will reach configurations that stabilize the charge distribution times the probability that the solute will jump to the intrinsic transition structure at the given solvent configuration.^{15a}

In Figure 5, the fluctuations of the solvent electric field in neutral glycine around its average value can be observed up to $t = 260$ fs. Fluctuations toward more positive values of the solvent electric field are expected to favor the proton transfer. Indeed, one may notice that the proton transfer begins when this electric field component reaches a local maximum. Solvent fluctuations are not the only cause which can induce proton transfer. One may also call upon geometric factors. For instance, the N–O2 distance which depends on several internal coordinates (bond distances, bond angles and dihedral angles) fluctuates around 2.5 Å. This distance between the proton donor and the proton acceptor atoms controls the intrinsic potential energy barrier for proton transfer: the more the distance shortens, the lower the barrier.³⁵ The curve for N–O2 distance is in a minimum when the proton transfer is produced. Note also that the N–H1 distance depends not only on the N–O2 distance but also on the N–H1–O2 angle. This angle oscillates between 130 and 140° before proton transfer but increases up to nearly 150° when the process occurs, leading to a diminution of the N–H1 distance. Besides these geometric factors, the energetics of the solute–solvent system must also be considered for explaining proton transfer. Interconversion between potential and kinetic energy as well as energy flow from the solvent to the solute may furnish the energy required to cross a hypothetical energy barrier.

4. Conclusions

We can conclude that the neutral glycine conformer studied here has a very small lifetime in water solution. It quickly undergoes transformation to the more stable zwitterionic species. The solvent plays an important role not only in the stabilization of the zwitterion but also in the proton transfer process, which is favored by convenient fluctuations of the environment. As we have pointed out, several other reactive trajectories have been computed, and, in general, the results parallel those presented in this paper, although one may note some differences, in particular for the correlation between solute and solvent dynamics. Obviously, general conclusions cannot be drawn without performing statistical averages, and the results presented in this paper must be understood subject to such limitations. It seems, however, that at the present level of calculation the free energy barrier of the glycine intramolecular proton transfer is not very high, because in every trajectory the system evolved toward the zwitterionic form after a few femtoseconds. In previous works,^{10–13} statistical analyses have been made using different approaches and reactions. In this way, it is possible to compute the transmission coefficient for the process which gives a clear idea of the importance of dynamic effects. The evaluation of nonequilibrium solvation contributions to the activation free energy would also require an appropriated treatment of solvent coordinates.³⁶ In the case of combined QM/MM molecular dynamics simulations, the computational cost of such an analysis is substantial, as can be deduced from the details given above. Nevertheless, it appears to be feasible. Thus, in a recent work, 140 trajectories have been simulated for a charge separation reaction (the first step in ethylene bromination) in aqueous solution, showing that the QM/MM technique is a powerful theoretical tool for investigating chemical processes in solution.²³

Acknowledgment. We thank F. R. Tortonda, J. L. Pascual-Ahuir, and J. Pitarch for helpful discussions, collaboration in the obtention of the structures, and technical assistance. I.T. acknowledges a postdoctoral contract of the Generalitat Valenciana. This work was partly supported by DGICYT Project PB96-0792, Spanish–French projects 267B and 96121, and by the Generalitat Valenciana Project GVD0C98-CB-11-8. Calculations were done on the computers of the Departamento de Química-Física (Valencia, Spain) with the assistance of W. Diaz and on the IBM SP2 of the CIRIL (Nancy, France).

References and Notes

- (1) (a) Albrecht, G.; Corey, R. B. *J. Am. Chem. Soc.* **1939**, *61*, 1087. (b) Jonsson, P. G.; Kvik, A. *Acta Crystallogr. B* **1972**, *28*, 1827–1833.
- (2) (a) Vishveshwara, S.; Pople, J. A. *J. Am. Chem. Soc.* **1977**, *99*, 2422–2426. (b) Sellers, H. L.; Schäfer, L. *J. Am. Chem. Soc.* **1978**, *100*, 7728–7729. (c) Schäfer, L.; Sellers, H. L.; Lovas, F. J.; Suenram, R. D. *J. Am. Chem. Soc.* **1980**, *102*, 6566–6568. (d) Hu, C. H.; Shen, M.; Schaefer, H. F., III. *J. Am. Chem. Soc.* **1993**, *115*, 2923–2930. (e) Császár, A. G. *THEOCHEM* **1995**, *346*, 141–152.
- (3) Ding, Y.; Krogh-Jespersen, K. *Chem. Phys. Lett.* **1992**, *199*, 261–266.
- (4) Jensen, J. H.; Gordon, M. S. *J. Am. Chem. Soc.* **1995**, *117*, 8159–8170.
- (5) (a) Tortonda, F. R.; Pascual-Ahuir, J. L.; Silla, E.; Tuñón, I. *Chem. Phys. Lett.* **1996**, *260*, 21–26. (b) Tortonda, F. R.; Pascual-Ahuir, J. L.; Silla, E.; Tuñón, I.; Ramirez, F. J. *J. Chem. Phys.* **1998**, *109*, 592–602.
- (6) Truong, T. N.; Stefanovich, E. V. *J. Chem. Phys.* **1995**, *103*, 3710–3717.
- (7) Okuyama-Yoshida, N.; Nagaoka, M.; Yamabe, T. *J. Phys. Chem. A* **1998**, *102*, 285–292.
- (8) (a) Cramer, C. J.; Truhlar, D. G. *Science* **1992**, *256*, 213–217. (b) Tomasi, J.; Persico, M. *Chem. Rev.* **1994**, *94*, 2027–2094. (c) Rivail, J. L.; Rinaldi, D.; Ruiz-López, M. F. In *Theoretical and Computational Models for Organic Chemistry*; Formosinho, S. J., Arnaut, L., Csizmadia, I., Eds.; Kluwer: Dordrecht, **1991**; pp 79–92.
- (9) (a) Romano, S.; Clementi, E. *Int. J. Quantum Chem.* **1978**, *14*, 839–850. (b) Clementi, E.; Cavallone, F.; Scordamaglia, R. *J. Am. Chem. Soc.* **1977**, *99*, 5531. (c) Carozzo, L.; Corongiu, G.; Petrongolo, C.; Clementi, E. *J. Chem. Phys.* **1978**, *68*, 787. (d) Alagona, G.; Ghio, C.; Kollman, P. *Theochem* **1988**, *166*, 385–392.
- (10) (a) Ciccotti, G.; Farrario, M.; Hynes, J. T.; Kapral, R. *J. Chem. Phys.* **1988**, *85*, 925. (b) Ciccotti, G.; Farrario, M.; Hynes, J. T.; Kapral, R. *J. Chem. Phys.* **1989**, *129*, 241. (c) Ciccotti, G.; Farrario, M.; Hynes, J. T.; Kapral, R. *J. Chem. Phys.* **1990**, *93*, 7137.
- (11) Keirstead, W. P.; Wilson, K. R.; Hynes, J. T. *J. Chem. Phys.* **1991**, *95*, 5256.
- (12) Hwang, J. K.; Creighton, S.; Warshel, A. *J. Am. Chem. Soc.* **1988**, *110*, 5297.
- (13) (a) Bergsma, J. P.; Gertner, B. J.; Wilson, K. R.; Hynes, J. T. *J. Chem. Phys.* **1987**, *86*, 1356. (b) Gertner, B. J.; Wilson, K. R.; Hynes, J. T. *J. Chem. Phys.* **1989**, *90*, 3537. (c) Gertner, B. J.; Whitnell, K. R.; Wilson, K. R.; Hynes, J. T. *J. Am. Chem. Soc.* **1991**, *113*, 74.
- (14) Warshel, A.; Weiss, R. M. *J. Am. Chem. Soc.* **1980**, *102*, 6218.
- (15) (a) Warshel, A. *J. Phys. Chem.* **1982**, *86*, 2218. (b) Hwang, J. K.; King, G.; Warshel, A. *J. Am. Chem. Soc.* **1988**, *110*, 5297. (c) Warshel, A. *Proc. Natl. Acad. Sci. U.S.A.* **1984**, *81*, 444.
- (16) (a) Warshel, A.; Levitt, M. *J. Mol. Biol.* **1976**, *103*, 227–249. (b) Gao, J.; Xia, X. *Science* **1992**, *258*, 631–635.
- (17) (a) Bash, P. A.; Field, M. J.; Karplus, M. *J. Am. Chem. Soc.* **1987**, *109*, 8092–8094. (b) Field, M. J.; Bash, P. A.; Karplus, M. *J. Comput. Chem.* **1990**, *11*, 700–733.
- (18) (a) Stanton, R. V.; Little, L. R.; Merz, K. M., Jr. *J. Phys. Chem.* **1995**, *99*, 17344–17348. (b) Freindorf, M.; Gao, J. *J. Comput. Chem.* **1996**, *17*, 386–395.
- (19) Stanton, R. V.; Hartsough, D. S.; Merz, K. M., Jr. *J. Phys. Chem.* **1993**, *97*, 11868–11870.
- (20) Tuñón, I.; Martins-Costa, M. T. C.; Millot, C.; Ruiz-López, M. F.; Rivail, J. L. *J. Comput. Chem.* **1996**, *17*, 19–29.
- (21) Tuñón, I.; Martins-Costa, M. T. C.; Millot, C.; Ruiz-López, M. F. *J. Mol. Model.* **1995**, *1*, 196–201.
- (22) Tuñón, I.; Martins-Costa, M. T. C.; Millot, C.; Ruiz-López, M. F. *J. Chem. Phys.* **1997**, *106*, 3633–3643.
- (23) Strnad, M.; Martins-Costa, M. T. C.; Millot, C.; Tuñón, I.; Ruiz-López, M. F.; Rivail, J. L. *J. Chem. Phys.* **1997**, *106*, 3643–3657.
- (24) (a) St-Amant, A.; Salahub, D. R. *Chem. Phys. Lett.* **1990**, *169*, 387–392. (b) Salahub, D. R.; Fournier, R.; Mlynarski, P.; Papai, I.; St-Amant,

A.; Ushio, J. In *Theory and Applications of Density Functional Approaches to Chemistry*; Labanowski, J., Andzelm, J., Eds.; Springer-Verlag: Berlin, 1991.

(25) Vosko, S. H.; Wilk, L.; Nusair, M. *Can. J. Phys.* **1980**, *58*, 1200–1211.

(26) (a) Becke, A. D. *Phys. Rev. A* **1988**, *38*, 3098–3100. (b) Perdew, J. P. *Phys. Rev. B* **1986**, *33*, 8822–8824. (c) Perdew, J. P. *Phys. Rev. B* **1986**, *34*, 7406–7406.

(27) Jorgensen, W. L.; Gao, J. *J. Phys. Chem.* **1986**, *90*, 2174–2182.

(28) Jorgensen, W. L.; Chandrashekar, J.; Madura, J. D.; Impey, R. W.; Klein, M. L. *J. Chem. Phys.* **1983**, *79*, 926–935.

(29) (a) Nosé, S. *Mol. Phys.* **1984**, *52*, 255–268. (b) Hoover, W. G.

Phys. Rev. **1985**, *31 A*, 1695–1697. (c) Nosé, S. *Mol. Phys.* **1986**, *57*, 187–191.

(30) Slifkin, M. A.; Ali, S. M. *J. Mol. Liq.* **1984**, *28*, 215–221.

(31) Mayer, I. *Chem. Phys. Lett.* **1983**, *97*, 270–274.

(32) Frank, H. S.; Wen, W. Y. *Discuss. Faraday Soc.* **1957**, *24*, 133.

(33) Kurz, J. L.; Kurz, L. C. *J. Am. Chem. Soc.* **1972**, *94*, 4451.

(34) (a) Marcus, R. A. *J. Phys. Chem.* **1968**, *72*, 891. (b) Kreevoy, M. M.; Konasewich, D. E. *Adv. Chem. Phys.* **1971**, *21*, 243.

(35) Scheiner, S. *Acc. Chem. Res.* **1985**, *18*, 174–180.

(36) (a) Muller, R. P.; Warshel, A. *J. Phys. Chem.* **1995**, *99*, 17516. (b) Ruiz-López, M. F.; Oliva, A.; Tuñón, I.; Bertrán, J. Submitted to *J. Phys. Chem.*